Leveraging Unlabeled Data for Glioma Molecular Subtype and Survival Prediction

Nicholas Nuechterlein, Beibin Li, Mehmet Saygin Seyfioğlu,
Sachin Mehta, Patrick J Cimino, and Linda Shapiro
University of Washington, Seattle
Email: {nknuecht, beibin, msaygin, sacmehta, shapiro}@cs.washington.edu pjjc@uw.edu

***Abstract*—In this paper, we address two long-standing challenges in glioma subtype and survival prediction: (1) how to leverage large amounts of unlabeled magnetic resonance (MR) imaging data and (2) how to unite MR data and genomic data. We propose a novel application of multi-task learning (MTL) that leverages unlabeled MR data by jointly learning an auxiliary tumor segmentation task with glioma subtype prediction and that can learn from patients with and without genomic data. We analyze multi-parametric MR data from 542 patients in the combined training, validation, and testing sets of the 2018 Multimodal Brain Tumor Segmentation Challenge and somatic copy number alteration (SCNA) data from 1090 patients in The Cancer Genome Atlas' (TCGA) lower-grade glioma and glioblastoma projects. Our MTL model significantly outperforms comparable classification models trained only on labeled MR data for both IDH1/2 mutation and 1p/19q co-deletion subtype prediction tasks. We also show that embeddings produced by our MTL model improve survival predictions beyond MR or SCNA on their own.**

I. Introduction

Gliomas make up 80% of all primary malignant brain tumors in adults [1]. The 2016 World Health Organization (WHO) criteria organizes diffuse gliomas into broad, survival-stratifying subtypes based on the mutation status of the genes IDH1 and IDH2 and the co-deletion status of whole chromosome arms 1p and 19q [2]. Although genomic markers are now the gold standard for glioma survival stratification, such data are only attainable via costly, invasive surgery. In contrast, magnetic resonance (MR) imaging is a safe, cost-effective, and readily available method that provides rich volumetric images of a patient's tumor.

Labeled glioma MR data have been used to predict IDH1/2 mutations [3]–[6], 1p/19q co-deletions [3], [7], and survival [8]–[12], but the potential utility of unlabeled data remains mostly unexplored. The Multimodal Brain Tumor Segmentation Challenges (BraTS) offer large datasets of public glioma MR data that have been used to train state-of-the-art 3D tumor segmentation models and pioneer open-source radiogenomic software [13]–[17]. Subtype and overall survival (OS) labels are available for a subset of patients in the 2018 BraTS dataset through The Cancer Genome Atlas (TCGA), but these labels are not available for most patients. Thus, training models only on labeled BraTS MR data leaves the bulk of these data unused. Similarly, genomic data in the TCGA is also available for this subset of BraTS patients. These genomic data have produced groundbreaking insights into glioma tumor biology [18]–[20] and should be used when available. Somatic copy number alteration (SCNA) data, which describe large, contiguous deletions or duplications of DNA, are particular interesting because their association with glioma subtype and survival is an evolving area of research [21]–[23].

Multi-task learning (MTL) is a machine learning strategy that allows models to learn multiple tasks simultaneously [24], [25]. Compared to single task learning, MTL allows models to learn richer data representations from more diverse data and labels by receiving feedback from complementary tasks [26], [27]. To allow MTL models to learn from unlabeled BraTS MR data, we exploit the recent advancements in brain tumor segmentation to assign weak segmentation labels to otherwise unlabeled MR samples.

In this paper, we propose a novel application of MTL that (1) jointly learns tumor segmentation with IDH1/2 or 1p/19q co-deletion subtype so that samples without subtype labels can contribute to model learning and (2) unites glioma genomic and imaging data by allowing SCNA data to serve as model input alongside MR data. Our MTL model that leverages unlabeled, 4-channel MR data accurately predicts IDH1/2 mutations (AUC = 0.89) and 1p/19q co-deletions (AUC = 0.87) and outperforms comparable 3D convolutional neural networks (CNNs) trained on labeled MR imaging data alone. Training with SCNA data dramatically boosts subtype performance (AUC $>$ 0.98) and raises the survival C-index score of survival models trained on embeddings generated by IDH1/2 prediction models from 0.719 to 0.735. To the best of our knowledge, this is the first MTL strategy that unites the BraTS MR and TCGA glioma SCNA datasets.

II. Methods

A. Dataset

Multi-parametric MR data were downloaded for 542 patients from the 2018 BraTS training, validation, and testing datasets. These MR data are 4-channel volumes composed of pre- (T1) and post-contrast

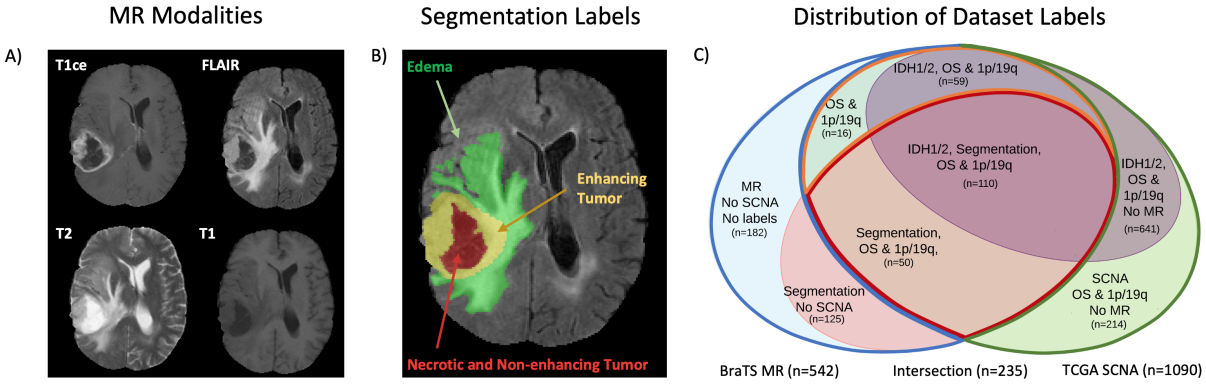

Fig. 1. **A)** Slices of four volumetric MR modalities of an IDH1/2 wildtype tumor in the BraTS dataset. Each MR sample is a 4-channel volume of dimension $4 \times 240 \times 240 \times 155$, where the 4 channels represent the T1ce, FLAIR, T2, and T1 MR modalities. The hallmark enhancing ring of aggressive tumors is clearly visible on the T1ce modality. **B)** A ground truth BraTS 4-class segmentation mask overlaid on the FLAIR modality with segmentation classes labeled. **C)** Distribution of labels in the merged BraTS and TCGA glioma SCNA datasets. The labeled training set is outlined with a red boundary; the validation set is outlined in a gold; the unlabeled MR data leveraged by our MTL model is outlined in blue; the set of samples with SCNA data but without MR data is outlined in green.

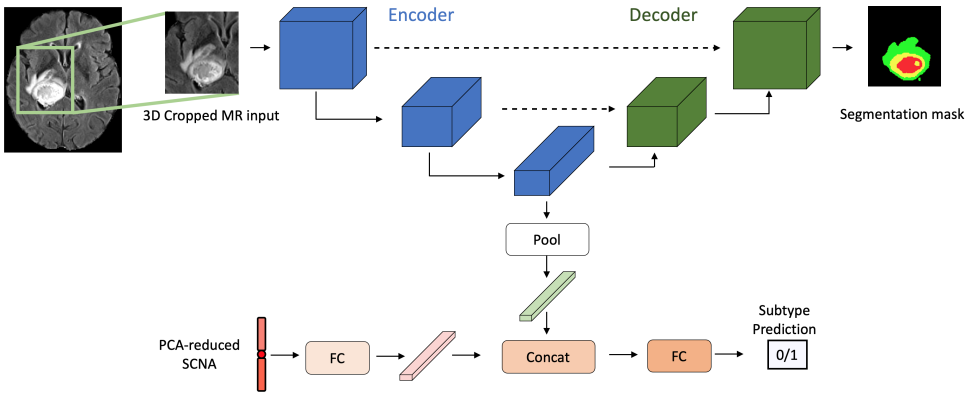

Fig. 2. Our MTL model uses the architecture of 3D-ESPNet [28] with a classification branch connected to the output of the encoder. PCA-reduced genomic SCNA data is passed though fully connected layers, concatenated with the average-pooled encoder output, and fed into a classifier to predict subtype class. The network decoder also produces a segmentation mask. We take the weighted cross-entropy loss of the subtype classification and tumor segmentation tasks. Our model accepts full brain multi-model MR volumes as well as cropped tumor volumes (shown here). We train models on 4-channel MR data input and 1-channel, single-modality input.

(T1ce) T1-weighted modalities and T2-weighted (T2) and T2 Fluid-Attenuated Inversion Recovery (FLAIR) modalities (Figure 1A). For 285 of the 542 BraTS patients, 4-class segmentation masks that denote three different tumor compartments and a background class (Figure 1B) are given. Gene-level SCNA data were downloaded for 1090 patients in the the TCGA lower-grade (WHO grade II/III) glioma and glioblastoma (WHO grade IV) projects from the University of California Santa Cruz cancer browser[1]. All 235 patients in the intersection of the BraTS MR dataset and the TCGA glioma SCNA dataset have overall survival (OS) and 1p/19q co-deletion labels, while only 171 have IDH1/2 labels. Of the 307 samples in the BraTS dataset with neither survival nor subtype labels, 125 have ground truth segmentation labels. We assign weak segmentation labels to the other 182 samples using a public, pre-trained tumor segmentation model [28]. The distribution of labels in our dataset is shown in Figure 1C.

[1]https://genome-cancer.ucsc.edu/

B. Multi-task learning

Model: Our MTL model is illustrated in Figure 2. The backbone of our network is an open-source ESPNet-based [28], [29] U-Net style [30] segmentation network pre-trained on the BraTS 2018 training dataset. To predict glioma subtype, we add a branch to the bottom of the network by average pooling the output of the network's encoder. To allow SCNA data to contribute to prediction, we pass 50-dimensional SCNA PCA embeddings though a small fully connected network and concatenate its output with the output of the average pooling step. We then pass this vector through a fully connected layer to obtain a binary IDH1/2 mutation or a binary 1p/19q co-deletion prediction.

Loss Function: For subtype classification, we take the weighted binary cross-entropy loss $\mathcal{L}_C$ for training samples that have subtype labels (Figure 1C, outlined in red) in addition to a variable segmentation loss. For training samples with 4-class ground truth segmentation labels (Figure 1C, red oval partially outlined in red), we take the weighted 4-class cross-entropy

Input Modalities	IDH1/2 Mutation (AUC)		1p/19q Co-deletion (AUC)		Overall Survival (C-index)	
	CNN	MTL (MR)	CNN	MTL (MR)	MTL (MR)	MTL (MR+SCNA)
All (Whole Brain)	0.669	**0.846**	0.605	**0.813**	0.587	**0.723**
All (Cropped)	0.872	**0.894**	0.744	**0.871**	0.697	**0.732**
T1ce (Cropped)	**0.893**	0.884	0.772	**0.819**	0.719	**0.735**
FLAIR (Cropped)	**0.778**	0.690	0.755	**0.818**	0.565	**0.731**
T1 (Cropped)	0.731	**0.738**	0.727	**0.757**	0.645	**0.728**
T2 (Cropped)	**0.778**	0.732	0.740	**0.755**	0.690	**0.718**
T1ce-T1 (Cropped)	**0.895**	0.861	**0.764**	0.742	0.707	**0.723**

TABLE I
RESULTS COMPARING MTL MODELS ACROSS PREDICTION TASKS AND MR INPUT FORMAT.

segmentation loss $\mathcal{L}_{S_{gt}}$ between the MTL model's decoder's output and the supplied segmentation mask. For unlabeled MR training samples for which 4-class segmentation labels are not available (Figure 1C, outer blue crescent), we take the weighted 2-class cross-entropy segmentation loss $\mathcal{L}_{S_{weak}}$ between the binarized output of the MTL model's decoder and the binarized weak segmentation mask supplied by the pre-trained segmentation network. We binarize our weak segmentation masks because whole tumor segmentation is known to be more reliable than within-tumor region segmentation for BraTS pre-trained models [17], [28]. Finally, we define our MTL loss as

$$\mathcal{L} = \mathcal{L}_C + \lambda \mathcal{L}_{S_{gt}} + (1-\lambda)\mathcal{L}_{S_{weak}} \quad (1)$$

where $\mathcal{L}_C$=0 for samples without subtype labels, and λ controls the feedback from weak and ground truth segmentation labels. For samples with ground truth segmentation labels, we set $\lambda = 1$. Otherwise, $\lambda = 0$.

We also train our MTL model on 1-channel, single modality MR input to assess the predictive power of each MR modality. When we train on T1-weighted modalities (T1ce, T1, T1ce-T1), we do not consider the edema segmentation label (Figure 1B) when evaluating $\mathcal{L}_{S_{gt}}$ because it is difficult to distinguish edema on these modalities. When we train on the T2 and FLAIR modalities, we binarized the tumor segmentation labels because these modalities characterize the tumor boundary better than any of the interior compartments. We do not modify $\mathcal{L}_{S_{weak}}$.

Survival Prediction: We perform survival regression analysis using a linear Cox Proportional Hazards (CPH) model trained on the last-layer embeddings produced by an MTL model pre-trained on the joint IDH1/2 mutation and tumor segmentation tasks [31]. We do not learn survival concurrently with subtype and tumor segmentation, because the CPH loss function requires large batch sizes that far exceed GPU memory given the size of 3D MR data (e.g., $> 200\times$ larger than ImageNet samples). We train our survival models on embeddings derived from the IDH1/2 mutation classification task rather than the 1p/19q co-deletion classification task because our IDH1/2 models are more accurate and IDH1/2 mutations stratify survival better than 1p/19q co-deletions [2].

III. EXPERIMENTAL RESULTS

Experiments: We first establish that utilizing unlabeled MR data boosts glioma subtype classification performance. To do this, we compare our MTL model trained with unlabeled MR data to 3D CNNs trained only on labeled MR data. For a fair comparison, we match the architecture of the CNNs with that of our MTL model's encoder and use the same hyperparameters. Second, we show that the performance of our MTL model improves when we allow for SCNA input. Third, we show that MR and SCNA data predict survival better than either on their own. To do this, we train linear CPH models on embeddings produced by MTL models trained on (1) MR data alone and (2) MR and PCA-reduced SCNA data and compare their results to those of a linear CPH model trained directly on PCA-reduced SCNA data. We perform these experiments with the following MR input formats:

- *All modalities (whole brain):* 4-channel volume consisting of all four MR modalities.
- *All modalities (cropped):* 4-channel volume consisting of all four MR modalities cropped to a tumor bounding box found using either ground truth or weak segmentation labels.
- *Single modalities (cropped):* Cropped 1-channel volumes consisting of a single MR modality.
- *T1ce-T1 modality (cropped):* Cropped 1-channel cropped volume constructed by subtracting the T1 volume from the T1ce volume. This volume accentuates the hallmark enhancing tumor region found on the T1ce modality (Figure 1A).

Evaluation Metrics and Training Details: For the IDH1/2 mutation and 1p/19q co-deletion prediction tasks, we report the average maximum area under curve (AUC) score for each model trained for 50 epochs over 10 trials. For survival prediction, we report the C-index, which measures the extent to which a model can properly order survival time. These are standard metrics in glioma MR-based classification and survival prediction [5]–[7], [32]–[34].

We split our MR dataset into 467 labeled and unlabeled MR training samples (Figure 1C, large oval outlined in blue and green) and 75 MR validation samples (Figure 1C, outlined in orange) defined by the intersection of the BraTS validation and testing

Input	1p/19q Co-del		IDH1/2 Mut, 1p/19q Intact		IDH1/2 Wildtype	
	MR	+SCNA	MR	+SCNA	MR	+SCNA
All (Wh. Br.)	0.714	**1.000**	0.606	**0.727**	0.487	**0.521**
All (Crop)	0.607	**0.964**	**0.742**	0.712	0.540	**0.548**
T1ce (Crop)	**0.821**	0.786	0.576	**0.742**	**0.644**	0.571
FLAIR (Crop)	0.607	**0.964**	0.636	**0.712**	0.527	**0.540**
T1 (Crop)	0.643	**0.893**	0.606	**0.636**	0.535	**0.544**
T2 (Crop)	**0.679**	0.500	**0.803**	0.697	0.562	**0.563**
T1ce-T1 (Cr.)	0.821	**0.857**	**0.803**	0.682	0.523	**0.552**
SCNA, PCA=5	0.929		0.667		0.512	

TABLE II
MTL SURVIVAL PERFORMANCE BROKEN UP OVER WHO 2016 GLIOMA SUBTYPES (C-INDEX).

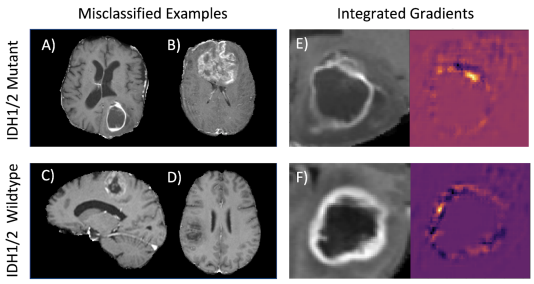

Fig. 3. Our T1ce-based IDH1/2 MTL network appears to associate tumor ring enhancement with IDH1/2 wildtype tumors. Sample **A-B, E)** are IDH1/2 mutant glioma with ring enhancement misclassified as IDH1/2 wildtype tumors. Samples **C-D)** are IDH1/2 wildtype tumors with mild and no enhancement misclassified as IDH1/2 mutants. Sample **F)** is a correctly classified IDH1/2 wildtype. Integrated gradients in the images to the right of **E)** and **F)** show that this model puts emphasis on tumor ring enhancement.

datasets with the TCGA glioma SCNA dataset. We use the remaining 855 samples with SCNA data but no MR data (Figure 1C, crescent outlined in green) to improve our SCNA PCA embeddings.

Subtype Results: Table I shows IDH1/2 mutation and 1p/19q co-deletion prediction results for models trained on the set of MR inputs detailed previously. The most dramatic boost MTL models give is on whole brain, all modality input, where they raise classification AUC by 0.18 for IDH1/2 mutation prediction and 0.21 for 1p/19q co-deletion prediction. Our MTL models almost ubiquitously outperform CNNs on the 1p/19q co-deletion task, but the results on the IDH1/2 task are less clear. We suspect that our MTL models do not significantly improve IDH1/2 prediction because both our best CNNs and MTL models are able to learn that tumor enhancement is strongly associated with IDH1/2 wildtype tumors: in the labeled training set, 85.5% of IDH1/2 wildtype tumors show strong enhancement and 83.6% of IDH1/2 mutant tumors show mild or no enhancement. A visualization of integrated gradients [35] and examples of incorrect IDH1/2 predictions in Figure 3 corroborate this explanation. Last, all MTL models trained with MR and SCNA data were able to classify IDH1/2 mutation and 1p/19q co-deletion status with AUC > 0.98. We leave these results out of Table I because they are too similar to compare.

Survival Results: The last columns of Table I show that embeddings produced by MTL models trained on SCNA and MR data better predict survival than embeddings produced by MTL models trained on MR data alone. In Table II, we break up our survival prediction results by WHO 2016 molecular subtype[2] and observe that these models perform exceptionally well on 1p/19q co-deleted tumors and offer some improvement for IDH1/2 wildtype gliomas. Our best MTL-embedding-based survival models also compare favorably to linear CPH models trained on PCA-reduced SCNA data alone, suggesting adding MR data to SCNA data improves survival prediction.

IV. DISCUSSION & CONCLUSION

Our primary contribution is a novel application of MTL that jointly learns glioma subtype and tumor segmentation, allowing MR data without subtype labels to contribute to learning. We show that using MTL to leverage these unlabeled MR data significantly improves 1p/19q co-deletion prediction. Additionally, we show that survival models trained on IDH1/2 MTL embeddings generally improve when SCNA data is added and that these models outperform survival models trained directly on SCNA PCA embeddings.

We observe that adding SCNA input to our MTL models drastically improves both subtype tasks (AUC > 0.98) across all MR inputs. This is likely explained by the facts that 1p/19q co-deletions are deductible from SCNA data and IDH1/2 wildtype tumors commonly carry distinctive SCNAs such as whole gain of chromosome 7 and whole loss of chromosome 10 [22]. On the other hand, links between SCNA data and patient survival are not as straightforward, and thus it is impressive that the inclusion of imaging data in our MTL-embedding-based survival models improves results set by survival models trained on SCNA data alone. Our observation that tumor enhancement plays a dominant role in the IDH1/2 prediction task demands that further experiments control for tumor enchantment, though the low count of IDH1/2 labels in the BraTS dataset presents a challenge.

We emphasize the clinical applications of this study. For patients who are unable to undergo brain surgery, or otherwise cannot obtain their IDH1/2 mutation and 1p/19q co-deletion status, accurate MR-based predictions of subtype place patients on different survival trajectories. For patients whose IDH1/2 mutation status and 1p/19q co-deletion status are known, our survival models offer the potential for sub-stratifying survival within glioma subtype. Improvements to survival stratification may lead to better treatment management, especially for predicted short-term survivors for whom early clinical trial enrollment may be recommended.

[2]All gliomas with 1p/19q co-deletions have IDH1/2 mutations.

ACKNOWLEDGMENTS

Nicholas Nuechterlein is supported by the National Science Foundation under Grant DGE-1762114.

REFERENCES

[1] M. L. Goodenberger and R. B. Jenkins, "Genetics of adult glioma," *Cancer genetics*, vol. 205, no. 12, 2012.

[2] D. N. Louis *et al.*, "The 2016 world health organization classification of tumors of the central nervous system: a summary," *Acta neuropathologica*, vol. 131, no. 6, 2016.

[3] Y. Matsui *et al.*, "Prediction of lower-grade glioma molecular subtypes using deep learning," *Journal of Neuro-Oncology*, vol. 146, no. 2, 2020.

[4] H. Arita, M. Kinoshita *et al.*, "Lesion location implemented magnetic resonance imaging radiomics for predicting idh and tert promoter mutations in grade ii/iii gliomas," *Scientific reports*, vol. 8, no. 1, 2018.

[5] X. Zhang, Q. Tian *et al.*, "Radiomics strategy for molecular subtype stratification of lower-grade glioma: detecting idh and tp53 mutations based on multimodal mri," *Journal of Magnetic Resonance Imaging*, vol. 48, no. 4, 2018.

[6] Z.-C. Li *et al.*, "Multiregional radiomics profiling from multiparametric mri: Identifying an imaging predictor of idh1 mutation status in glioblastoma," *Cancer medicine*, vol. 7, no. 12, 2018.

[7] P. Chang *et al.*, "Deep-learning convolutional neural networks accurately classify genetic mutations in gliomas," *American Journal of Neuroradiology*, vol. 39, no. 7, 2018.

[8] K. E. Emblem *et al.*, "Machine learning in preoperative glioma mri: Survival associations by perfusion-based support vector machine outperforms traditional mri," *Journal of magnetic resonance imaging*, vol. 40, no. 1, 2014.

[9] P. Kickingereder, S. Burth *et al.*, "Radiomic profiling of glioblastoma: identifying an imaging predictor of patient survival with improved performance over established clinical and radiologic risk models," *Radiology*, vol. 280, no. 3, 2016.

[10] P. Kickingereder, U. Neuberger *et al.*, "Radiomic subtyping improves disease stratification beyond key molecular, clinical, and standard imaging characteristics in patients with glioblastoma," *Neuro-oncology*, vol. 20, no. 6, 2018.

[11] X. Liu *et al.*, "A radiomic signature as a non-invasive predictor of progression-free survival in patients with lower-grade gliomas," *NeuroImage: Clinical*, vol. 20, 2018.

[12] Q. Li *et al.*, "A fully-automatic multiparametric radiomics model: towards reproducible and prognostic imaging signature for prediction of overall survival in glioblastoma multiforme," *Scientific reports*, vol. 7, no. 1, 2017.

[13] K. Kamnitsas *et al.*, "Deepmedic for brain tumor segmentation," in *International workshop on Brainlesion: Glioma, multiple sclerosis, stroke and traumatic brain injuries*. Springer, 2016.

[14] S. Rathore, S. Bakas *et al.*, "Brain cancer imaging phenomics toolkit (brain-captk): an interactive platform for quantitative analysis of glioblastoma," in *International MICCAI Brainlesion Workshop*. Springer, 2017.

[15] B. H. Menze *et al.*, "The multimodal brain tumor image segmentation benchmark (brats)," *IEEE transactions on medical imaging*, vol. 34, no. 10, 2014.

[16] S. Bakas, H. Akbari, A. Sotiras *et al.*, "Advancing the cancer genome atlas glioma mri collections with expert segmentation labels and radiomic features," *Scientific data*, vol. 4, 2017.

[17] S. Bakas *et al.*, "Identifying the best machine learning algorithms for brain tumor segmentation, progression assessment, and overall survival prediction in the brats challenge," *arXiv preprint arXiv:1811.02629*, 2018.

[18] C. G. A. R. Network *et al.*, "Comprehensive genomic characterization defines human glioblastoma genes and core pathways," *Nature*, vol. 455, no. 7216, p. 1061, 2008.

[19] R. G. Verhaak *et al.*, "Integrated genomic analysis identifies clinically relevant subtypes of glioblastoma characterized by abnormalities in pdgfra, idh1, egfr, and nf1," *Cancer cell*, vol. 17, no. 1, pp. 98–110, 2010.

[20] H. Noushmehr *et al.*, "Identification of a cpg island methylator phenotype that defines a distinct subgroup of glioma," *Cancer cell*, vol. 17, no. 5, pp. 510–522, 2010.

[21] P. J. Cimino *et al.*, "Copy number profiling across glioblastoma populations has implications for clinical trial design," *Neuro-oncology*, vol. 20, no. 10, pp. 1368–1373, 2018.

[22] D. J. Brat, K. Aldape, H. Colman, E. C. Holland, D. N. Louis, R. B. Jenkins, B. Kleinschmidt-DeMasters, A. Perry, G. Reifenberger, R. Stupp *et al.*, "cimpact-now update 3: recommended diagnostic criteria for "diffuse astrocytic glioma, idh-wildtype, with molecular features of glioblastoma, who grade iv"," *Acta neuropathologica*, vol. 136, no. 5, pp. 805–810, 2018.

[23] D. J. Brat, K. Aldape, H. Colman, D. Figrarella-Branger, G. N. Fuller, C. Giannini, E. C. Holland, R. B. Jenkins, B. Kleinschmidt-DeMasters, T. Komori *et al.*, "cimpact-now update 5: recommended grading criteria and terminologies for idh-mutant astrocytomas," *Acta neuropathologica*, vol. 139, no. 3, pp. 603–608, 2020.

[24] R. Caruana, "Multitask learning," *Machine learning*, vol. 28, no. 1, pp. 41–75, 1997.

[25] T. Evgeniou and M. Pontil, "Regularized multi–task learning," in *Proceedings of the tenth ACM SIGKDD international conference on Knowledge discovery and data mining*, 2004.

[26] K. He *et al.*, "Mask r-cnn," in *Proceedings of the IEEE international conference on computer vision*, 2017.

[27] E. Hajiramezanali, S. Z. Dadaneh, A. Karbalayghareh, M. Zhou, and X. Qian, "Bayesian multi-domain learning for cancer subtype discovery from next-generation sequencing count data," in *Advances in Neural Information Processing Systems*, 2018, pp. 9115–9124.

[28] N. Nuechterlein and S. Mehta, "3D-ESPNet with pyramidal refinement for volumetric brain tumor image segmentation," in *International MICCAI Brainlesion Workshop*. Springer, 2018.

[29] S. Mehta *et al.*, "ESPNet: Efficient spatial pyramid of dilated convolutions for semantic segmentation," in *Proceedings of the european conference on computer vision (ECCV)*, 2018.

[30] O. Ronneberger *et al.*, "U-net: Convolutional networks for biomedical image segmentation," in *International Conference on Medical image computing and computer-assisted intervention*. Springer, 2015.

[31] D. R. Cox, "Regression models and life-tables," *Journal of the Royal Statistical Society: Series B (Methodological)*, vol. 34, no. 2, pp. 187–202, 1972.

[32] Z. Li *et al.*, "Deep learning based radiomics (dlr) and its usage in noninvasive idh1 prediction for low grade glioma," *Scientific reports*, vol. 7, no. 1, 2017.

[33] C. Su, J. Jiang *et al.*, "Radiomics based on multicontrast mri can precisely differentiate among glioma subtypes and predict tumour-proliferative behaviour," *European radiology*, vol. 29, no. 4, 2019.

[34] J. Lao *et al.*, "A deep learning-based radiomics model for prediction of survival in glioblastoma multiforme," *Scientific reports*, vol. 7, no. 1, 2017.

[35] M. Sundararajan *et al.*, "Axiomatic attribution for deep networks," in *Proceedings of the 34th International Conference on Machine Learning-Volume 70*. JMLR. org, 2017.